Meteoritics & Planetary Science 57, Nr 8, 1617–1626 (2022)
doi: 10.1111/maps.13829

Report

Thermal conductivity of basalt between 225 and 290 K

D. HALBERT* and J. PARNELL

School of Geosciences, University of Aberdeen, King's College, Meston Building, Aberdeen, AB24 3UE, UK
*Corresponding author. E-mail: d.halbert@abdn.ac.uk

(Received 12 October 2021; revision accepted 25 April 2022)

Abstract–Thermal conductivity of natural rock is only well characterized for temperatures above 273 K, i.e., at typical Earth values. In planetary science, there is a requirement to explore the thermal characteristics of rock at temperatures below 273 K, for which thermal conductivity data are sparse or contested. Here, we present empirical data for a basalt showing thermal conductivity ranging from 2.71 ± 0.09 W m^{-1} K^{-1} at 224.4 K, to 2.63 ± 0.05 W m^{-1} K^{-1} at 288.8 K. Previous work reports much lower values in this range, which may be due to the fragmented nature of the previous research, the use of powdered samples for some data, and the effect of porosity. The high-temperature thermal conductivity laws of Sass et al. (1992) and Haenel and Zoth (1973) can be robustly extrapolated to cover the temperature range of our data.

INTRODUCTION

Thermal conductivity is a critical parameter for describing the ability of heat to flow through a substance. Thermal conductivity is temperature dependent for solids and has been widely measured for a range of materials, including common rock types. Measurements of thermal conductivity for rock normally take as a lower temperature; either room temperature (variously described), or 0°C. This is expected, with only a few exceptions, such as in the polar regions and at high altitudes, where rock on Earth is at temperatures above 0°C, there is little scientific or industrial need to derive subzero thermal conductivity measurements of natural rock. With many thermal conductivity measurements of different rocks at various temperatures, it is possible to construct general laws for the temperature dependence of thermal conductivity in various rock types. These laws are constrained by their data to a valid range for which the lower limit is at or above 0°C.

Elsewhere in the solar system, the situation is different. Mars, with an average surface temperature of around 210 K, has significant portions of its crust at subzero temperatures. The Moon and other small bodies also have low-temperature rock.

Lunar research has provided some data on low-temperature conductivity; however, there are significant caveats on its use. Most research that has been done on regolith and bulk rock research has not determined the thermal conductivity directly, but rather calculated it from diffusivity, specific heat capacity, and density data. These data have been corralled from a variety of sources and have some limitations, such as the use of powdered samples to determine some data (possibly as a method to overcome porosity). Overall, they show thermal conductivities lower than expected by theory or extrapolation from measurements made at higher temperatures.

In the frame of Antarctic research some measurements have been made, that is, Nagao and Kaminuma (1986), although none of the rocks studied were basalts, and work has been done on the thermal conductivities of basaltic meteorites (Opeil et al., 2012).

Given the scarcity of thermal conductivity data on rocks at subzero temperatures, and the need for such data to inform planetary science, we have conducted an experiment to determine the thermal conductivity of a basalt sample at temperatures between approximately 225 and 290 K, the limits of our equipment.

METHOD

We use the "divided bar" method (Beck & Beck, 1958) to determine thermal conductivity for a basalt sample over a temperature range from 224.4 to

288.8 K in steps of about 5 K representing multiple measurements at 17 different temperatures.

The sample is a fine-grained basalt from the pyroxenitic zone of the Theo's Flow Formation in Ontario, Canada (Arndt & Nesbitt, 1982). This sample was chosen for its homogeneity; absence of layering; and for its composition, which is similar to the nakhlite meteorites from Mars (Lentz et al., 2011), although it should not be seen as fully representative of Martian meteorites. See McSween (2015) for an overview of the variability of Martian meteorites.

The sample has a density of 3033 kg m^{-3} and an effective porosity of zero percent, measured by the resaturation method.

A reference sample with a known thermal conductivity (crystalline quartz) was placed in series with the sample and a heat flow applied across both. The thermal conductivity of the sample is then derived without knowing the heat input across the sample through the equation:

$$\lambda_s = \lambda_r \frac{A_r \Delta T_r L_s}{A_s \Delta T_s L_r}, \quad (1)$$

where i is the cross section, ΔT is the change in temperature between temperature sensors, and L is the distance between temperature sensors; the subscripts distinguish between the sample and reference.

The apparatus consists of a copper bar, 30 mm in diameter, with two divisions into which the quartz reference and the sample were inserted. A Kapton heater was attached to one end of the bar and a Peltier cooling module at the other so that a steady heat flow along the bar could be established. A thin layer of thermally conductive paste was used for the interfaces between the bar, the inserts, and the heating/cooling elements. Four type K thermocouples were placed into holes in the bar on either side of the reference and sample, again with a thin layer of conductive paste to provide an interface (Fig. 1).

The quartz reference is a lab-grown crystalline quartz disk sourced from VM-TIM GmbH. The z-axis is orientated perpendicular to the disk faces. The dimensions are 30 mm diameter and 12 mm thickness, a ratio of 2.5.

The values of thermal conductivity for crystalline quartz, with heat flow parallel to the c-axis, were taken from a reference table (Touloukian et al., 1970). The values appropriate for the temperature range were fitted to a polynomial. The polynomial fit has a chi-square of 0.0005. The reference values are stated to be within 5% to 10% of the true value, an uncertainty which flows through the calculation to the final thermal conductivity values.

The basalt sample was cut to match the dimensions of the reference. The disk faces are parallel to within 0.01 mm and match the dimensions of the crystalline reference to within 0.05 mm.

The entire apparatus was placed into a standard laboratory −80° freezer, in a vertical orientation with the heater uppermost, and the front panel temperature setting decreased from 0°C to −80°C in steps of 5°. The four thermocouples were connected to a Data-scan 7321 data-logger and readings were taken every 5 s. A typical run at each temperature setting took 3 h to ensure that a steady state had been achieved and that any latent heat effects had stabilized as no humidity control was possible. In practice, the temperature varied in a roughly sinusoidal manner of around 2–3 K as the freezer went through an on–off cycle.

As there is a lag in the heat flow response when temperature is climbing or falling leading to an erroneous reading, the first derivative of the data was calculated, and the data points were used only where the derivative was close to zero (±0.001).

Radiative and convective losses from the stack were compensated for mathematically. The Stefan–Boltzmann law was used to calculate the radiation loss:

$$Q = \epsilon \sigma A \left(T_S^4 - T_A^4\right), \quad (2)$$

where Q is the radiated power, ε is the emissivity, σ is the Stefan–Boltzmann constant, and A is the emitting area. The subscripts S and A indicate the surface and ambient temperatures, respectively. The emissivity values used were crystalline quartz, 0.89; and basalt, 0.72 (Gubareff et al., 1960). Both values are for room temperature as no values for lower temperatures are known. For copper, some data exist for emissivity at lower temperatures. A value of 0.023, appropriate to 250 K, was used (Frolec et al., 2019).

The convective heat losses were calculated using the equation:

$$Q = hA(T_S - T_A), \quad (3)$$

where Q is the total heat transfer, h is the convective heat transfer coefficient, and A is the surface area. The subscripts S and A indicate the surface and ambient temperatures, respectively. The calculation of h for a laminar flow is (Churchill & Chu, 1975)

$$h = \frac{k_{air}}{L}\left(0.68 + \frac{0.67 Ra^{1/4}}{\left[1 + (0.437/Pr)^{9/16}\right]^{4/9}}\right), \quad (4)$$

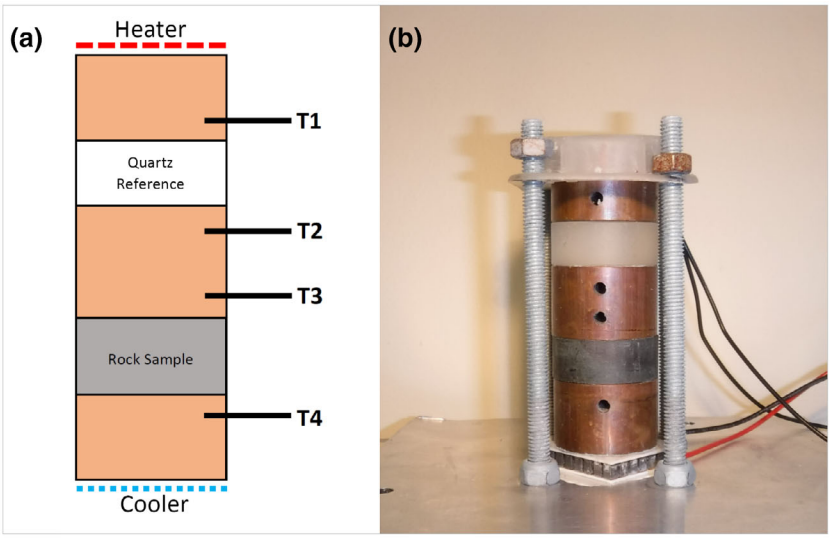

Fig. 1. Schematic diagram and photograph of the apparatus. The apparatus is a copper cylindrical bar with a quartz reference insert and an identically sized rock sample insert. The distance between the thermocouples T1 and T2 is identical to the distance between T3 and T4. The holes into which the thermocouples were inserted can be seen in the photograph. The Peltier cooler can be seen at the bottom and the wires for the Kapton heater can be seen leading into the top of the stack. The screw clamps were used to keep the apparatus together and provide enough force to ensure a good contact between the components. (Color figure can be viewed at wileyonlinelibrary.com.)

where k_{air} is the thermal conductivity of air, L is the characteristic length, Ra is the Rayleigh number, and Pr is the Prandtl number. The thermal conductivity of air and the Prandtl number vary with temperature; values were extrapolated from reference tables (Çengel, 2009). The same tables were used to source the value of the kinematic viscosity of air used to calculate the Rayleigh number. The value of the coefficient of thermal expansion of air, also used to calculate the Rayleigh number, used the ideal gas approximation $1/T$. The vertical dimension was used as the characteristic length.

RESULTS

Thermal conductivity in the sample was determined to be around 2.6 W m^{-1} K^{-1}, ranging from 2.71 ± 0.09 W m^{-1} K^{-1} at 224.4 K, the lowest temperature measured, to 2.63 ± 0.05 W m^{-1} K^{-1} at 288.8 K, the highest temperature. The average, upper, and lower range of the thermal conductivity values were recorded for each run and are presented in Table 1.

Table 1. Thermal conductivity of a basalt sample at a range of low temperatures.

Temperature (K)	Average (W m^{-1} K^{-1})	Range (W m^{-1} K^{-1})
224.4	2.71	+0.06, −0.09
225.2	2.70	+0.04, −0.07
230.0	2.67	+0.04, −0.06
232.6	2.71	+0.04, −0.07
236.5	2.71	+0.05, −0.06
240.5	2.71	+0.03, −0.07
244.5	2.71	+0.03, −0.05
249.8	2.67	+0.05, −0.07
254.0	2.68	+0.03, −0.05
258.0	2.68	+0.04, −0.07
263.7	2.63	+0.03, −0.05
268.0	2.61	+0.03, −0.03
271.9	2.62	+0.03, −0.07
276.3	2.60	+0.03, −0.06
281.1	2.61	+0.03, −0.04
284.6	2.63	+0.07, −0.08
288.8	2.63	+0.05, −0.05

DISCUSSION

Previous Work on Low-Temperature Thermal Conductivity

Previous attempts by others were made to derive low-temperature thermal conductivity for basalts, but the values obtained are sparse, derived in a disconnected way, and difficult to reconcile with theory. It was the inadequacy of these data that served as the motivation for this work. Several low-temperature data sets arose from the Apollo program, particularly from Apollo 11 and 12, which measured thermal diffusivity and then derived thermal conductivity. The Apollo 11 rocks (with sample numbers 10xxx) have a high K and high Ti (typically around 10%) and low SiO_2 composition compared with our sample.

As the thermal conductivity of quartz is 7.70 W m^{-1} K^{-1}, orthoclase 2.32 W m^{-1} K^{-1}, and plagioclase 2.15 W m^{-1} K^{-1} (all from Horai, 1971), we could expect our sample to have slightly higher thermal conductivity than the lunar samples.

Fujii and Osako (1973) measured thermal diffusivity for lunar samples 10049 and 10069 and an alkaline olivine terrestrial basalt from 60 to 820 K to derive a temperature-dependent relationship between temperature and thermal diffusivity:

$$\kappa = A + \frac{B}{T} + C \times T^3, \tag{5}$$

where A, B, and C are parameters fitted separately for each of the three rocks and T is in °C. A least-squares fit from the specific heat capacity data of Robie et al. (1970) for a lunar sample 10057 (a different rock) was then used to determine thermal conductivity.

Later, Horai and Fujii (1972) used these specific heat data supplemented by diffusivity data from additional rocks (lunar samples 10020, 10046, 10057, and 10065). It was observed that the variation in thermal conductivity for these lunar samples was relatively small at temperatures above 200 K, and that below 200 K, the thermal conductivity decreases monotonically toward zero. The authors warn that the specific heat data used are not in accordance with the Debye theory of thermal conductivity (see Tritt [2012] and others for a description of this theory).

Lunar sample 10057 is the only rock with empirical diffusivity (Horai et al., 1970), specific heat capacity (from powdered samples, not bulk rock; Robie et al., 1970), and density measurements (LSPET, 1969); therefore, a calculation of the thermal conductivity is possible. This was done by Robie and Hemingway (1971). The values, between 1.6 and 2.1 W m^{-1} K^{-1}, show no correlation with temperature over the range 149–436 K.

There are significant limitations to the thermal conductivity values derived from lunar samples, which were calculated indirectly from diffusivity, specific heat capacity, and density data, from a wide variety of disparate rocks, and combined measurements from bulk and powdered samples. For the most part, the lunar data show a consistent profile between 200 and 300 K of a flat, or slightly descending, profile with decreasing temperature (Fig. 2a). This profile is unexpected as theory indicates that thermal conductivity should slightly increase with decreasing temperature in this range (see Tritt, 2012).

The thermal conductivities of basaltic meteorites, including a shergottite (Los Angeles) attributed to Mars and a howardite (Frankfort) attributed to Vesta, in the range 200 K to 300 K are much lower (below 1.0W m^{-1} K^{-1}) than expected for basalt (Opeil et al., 2012). A strong linear relationship between thermal conductivity at 200 K and the inverse of the porosity suggests that their data are strongly controlled by porosity and microfractures rather than the bulk conductivity of the rock.

In addition to the lunar and meteoritic samples, basalt from Dresser, Wisconsin has also been tested at low temperature (Marovelli & Veith, 1965). Three measurements were taken at 208, 254, and 298 K, of a sample referred to as block E. The values are much higher than for the lunar samples and slightly higher than for these new data. Another sample (block B) gave values compatible with the lunar samples. The authors consider these two samples high and low outliers due to their visible differences to their other samples (blocks A, C, and D) but indicative of an expected range for basaltic rocks.

Extrapolation of High-Temperature Thermal Conductivity Values

While data on low-temperature thermal conductivity are sparse, there are many thermal conductivity measurements on terrestrial rocks at temperatures above 273 K and some general laws for the temperature dependence of thermal conductivity at these temperatures have been proposed. We assess if it is possible to extrapolate any of the high-temperature relationships to fit our low-temperature data.

A general law proposed by Haenel and Zoth (1973), and valid from 273 to 1473 K, for any rock type is

$$\lambda(T) = 3.6 - 0.49 \times 10^{-2} T + 0.61 \times 10^{-5} T^2 - 2.58 \times 10^{-9} T^3, \tag{6}$$

where λ is the thermal conductivity and T is in K. Subsequently, Zoth and Haenel (1988) derived an equation specifically for basalt:

$$\lambda(T) = \frac{474}{350 + T} + 1.181, \tag{7}$$

where T is in °C, valid for 323 to 1073 K. This relationship was adopted in a standard reference handbook (Clauser & Huenges, 1995) and is widely used in planetary research. In a further refinement, a method to determine thermal conductivity at a given temperature if the thermal conductivity at room temperature is known has been developed by Sass et al. (1992),

$$\lambda(T) = \frac{\lambda_{273\mathrm{K}}}{1.007 + T\left(0.0036 - \frac{0.0072}{\lambda_{273\mathrm{K}}}\right)}, \tag{8}$$

where T is in °C and the equation is valid for the range 273–473 K.

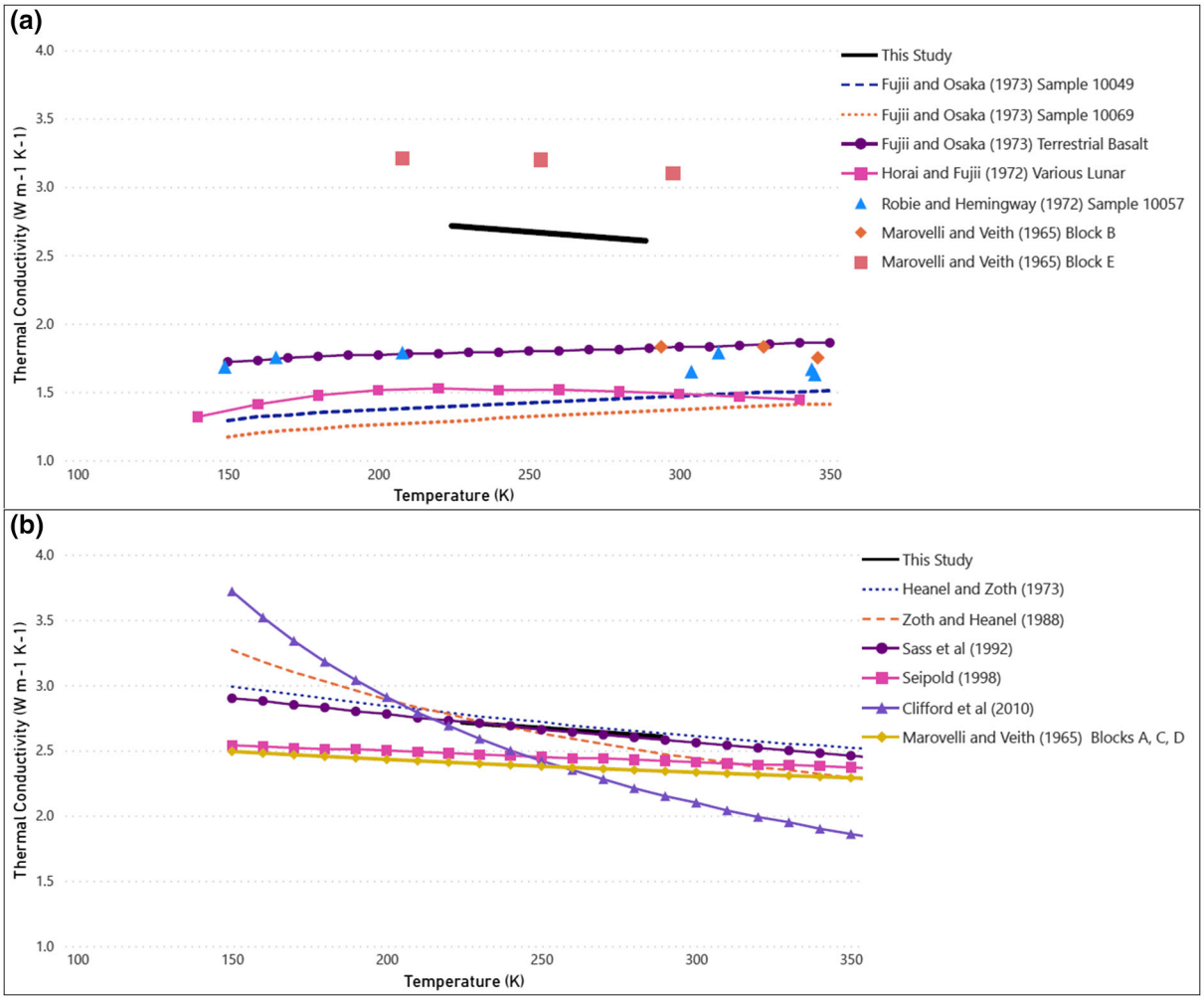

Fig. 2. Comparison of the new thermal conductivity data with other thermal conductivity data sets. a) Comparison with data determined from returned lunar samples and some terrestrial basalts. b) Comparison with extrapolations of high-temperature general laws for the relationship between temperature and thermal conductivity. (Color figure can be viewed at wileyonlinelibrary.com.)

A more recent general law for the temperature dependence of thermal conductivity was proposed by Seipold (1998) and is

$$\lambda = \frac{1}{(B \times (T - 532 \pm 45) + 0.448 \pm 0.014)}, \quad (9)$$

where T is in K and B is a parameter related to rock type. For basalts, B is $1.43 \times 10^{-4} \pm 1.00$. The equation is valid in the range 273–873 K.

It is also possible to construct a curve through blocks A, C, and D of the Marovelli and Veith (1965) data,

$$\lambda = \frac{1.73}{0.6272 + (2.965 \times 10^{-4} \times 1.8T) - (2.067 \times 10^{-7} \times 1.8T^2)}. \quad (10)$$

If Equations 6–10 are extrapolated to lower temperatures, they can be compared to the results of our new experiment (Fig. 2b).

The extrapolations are in broad agreement with the new experimental data. Equation 6 parallels the slope of the experimental data closely and can be used with caution. The general law described by Equation 7 has a steeper slope but intersects the experimental data at around 250 K. Equations 9 and 10 are less consistent with the general trends described by Equations 7 and 8 and our data. The general law described by Equation 8 provides the closest match.

An approach that has been used to model thermal conductivity of the Martian crust is to assume an ice-saturated basaltic composition for a significant portion of the crust. Given that at higher temperatures the profile of the thermal conductivity of water ice is similar

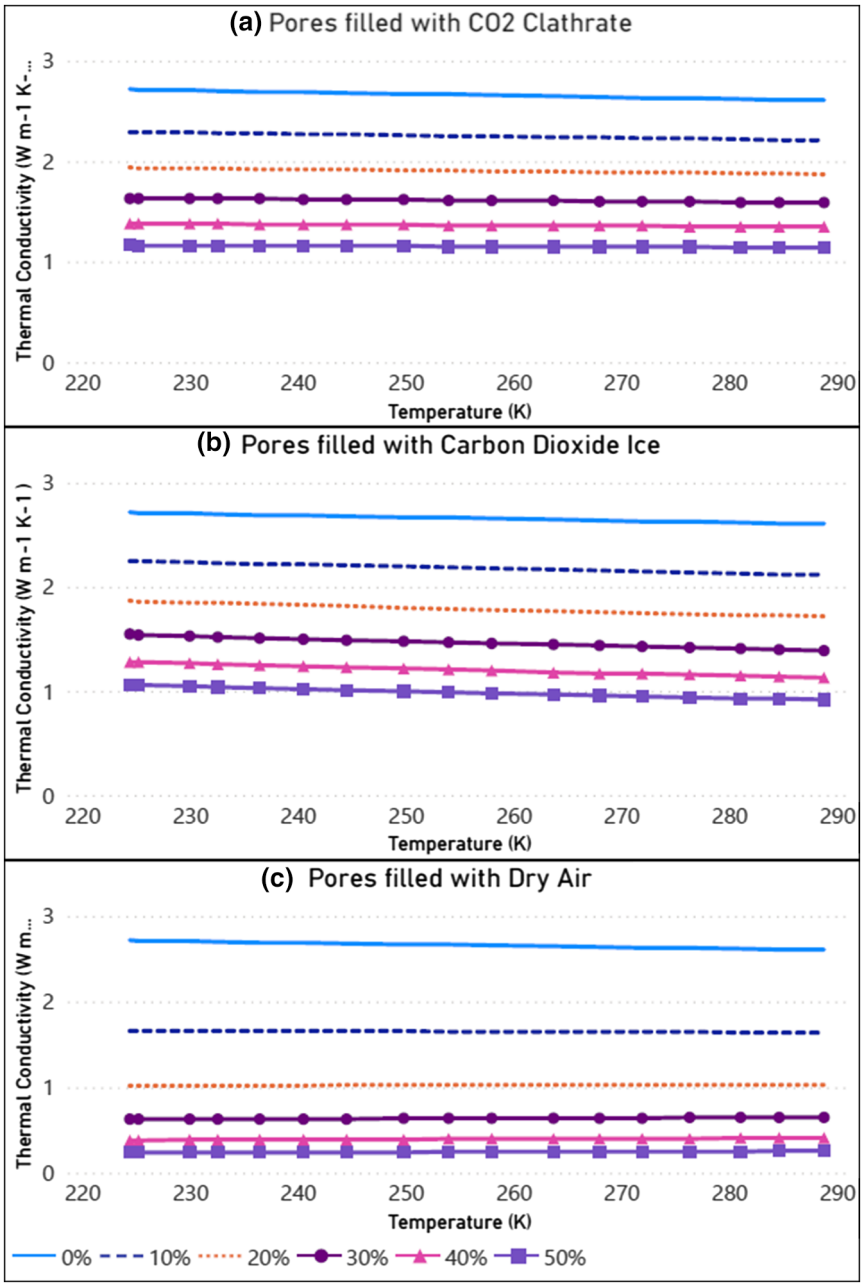

Fig. 3. Calculations of the thermal conductivity of basalt of various porosities and varying pore-filling substances. The calculations used the geometric mean mixing law (Equation 14) and the thermal conductivity values for basalt from this paper, CO_2 clathrate from Sloan (1997), CO_2 ice from Kravchenko and Krupskii (1986), and dry air from Kadoya et al. (1985). (Color figure can be viewed at wileyonlinelibrary.com.)

to that of basalt, the water ice values are used to model conductivity of the crust irrespective of the basalt/ice ratio expected (Clifford et al., 2010). The thermal conductivity profile of water ice (Hobbs, 1974), used as a proxy for a basalt/ice combination,

$$\lambda = \frac{488.19}{T} + 0.4685, \tag{11}$$

has also been plotted on Fig. 2b. It has low correlation with the new data.

Effects of Porosity

The thermal conductivity of a porous rock can be treated as a combination of the thermal conductivities of the two components: the solid phase and the pore-

Table 2. Porosity of some samples referenced in this paper and the thermal conductivity of our sample assuming the same porosity.

Sample	Porosity	Reference	Thermal conductivity of our sample for the same porosity (W m^{-1} K^{-1})
10049	5.65%	Fujii and Osako (1973)	2.01–2.06
10069	11.0%	Fujii and Osako (1973)	1.57–1.59
Terr. Sample	4.8%	Fujii and Osako (1973)	2.09–2.05
10057	17.4%	Kanamori et al. (1970)	1.16–1.17
"Frankfort"	12.7%	Macke et al. (2010)	1.45–1.46
"Los Angeles"	8.1%	Macke et al. (2010)	1.79–1.83

filling phase. The thermal conductivity of water, water ice, CO_2, CO_2 ice, and CO_2 clathrates, the most likely pore-filling substances in a planetary context, are well characterized at low temperatures. The sample used in this experiment, having a porosity of zero, is thus ideal to provide a solid phase thermal conductivity allowing an estimation of the bulk effective thermal conductivity to be made for any given porosity.

Several mixing laws exist to predict the effective thermal conductivity of a multi-component mixture; for example, Beardsmore and Cull (2001) suggest the following:

$$\frac{1}{\lambda_{\text{eff}}} = \sum_{i=1}^{n} \frac{\phi_i}{\lambda_i} \quad \text{Harmonic Mean} \tag{12}$$

$$\lambda_{\text{eff}} = \sum_{i=1}^{n} \phi_i \lambda_i \quad \text{Arithmetic Mean} \tag{13}$$

$$\lambda_{\text{eff}} = \prod_{n=1}^{n} \lambda_i^{\phi_i} \quad \text{Geometric Mean} \tag{14}$$

where each component i has a thermal conductivity λ and a percentage ϕ. The harmonic mean can be visualized as a series of layers perpendicular to the heat flow, such as bedding layers, and the arithmetic mean a series of layers parallel with the heat flow, such as vertical dykes. The geometric mean is suitable for a mixed situation such as a porous rock. The harmonic mean is sensitive to the lowest thermal conductivity component and the arithmetic mean to the highest conductivity component; therefore, for any given mixture, they provide the lower and upper (Wiener's) bounds, respectively.

Applying the above equations to our zero-porosity sample allows an estimate to be made of the thermal conductivity of basalt crust with varying porosity, and for several possible pore-filling materials. In Fig. 3, we present calculations of a geometric mean thermal conductivity for a variety of porosities and pore-filling substances. For a CO_2 clathrate, the value of 0.5 W m^{-1} K^{-1} is taken from Sloan (1997). The thermal conductivities of CO_2 ice and dry air are temperature dependent and are calculated according to the methods of Kravchenko and Krupskii (1986) and Kadoya et al. (1985), respectively.

Calculating the effects of porosity in the case of dry air as in Fig. 3c can give insights into the lunar and meteoritic data. Assuming that the thermal conductivity measurements of the meteoritic and lunar samples were taken with dry samples in air with standard sea-level pressure and density, we can calculate the thermal conductivity of our sample for the same porosity using the method of Kadoya et al. (1985) and then compare it to the measured thermal conductivities of the lunar and meteoritic samples from Fig. 2a. We have porosities for six of the samples referenced in this paper. Table 2 shows the samples we have porosity information for, and a calculated thermal conductivity for our sample assuming the same porosity.

All the samples of Fujii and Osako (1973) show considerably lower thermal conductivities than our sample would for the same porosity; however, sample 10057, used by Horai and Fujii (1972) and Robie and Hemingway (1971) shows somewhat higher values than our sample would at the same porosity. This could be a feature of the use of powdered material in the thermal conductivity measurements using this sample. If loosely packed, powdered material exhibits a low thermal conductivity measurement, but if tightly packed, powdered samples can be used to lessen the problem of high porosity. Given the combining of data from different rocks in the lunar work, it is not possible to go beyond a broad statement that porosity is likely to be one of the reasons the lunar data show values consistently lower than this paper.

The thermal conductivity of the two meteoritic samples, measured by Opeil et al. (2012) to be below 1.0 W m^{-1} K^{-1}, are lower than the corresponding values for our sample. This could be due to the presence, noted by Opeil et al. (2012), of microfractures.

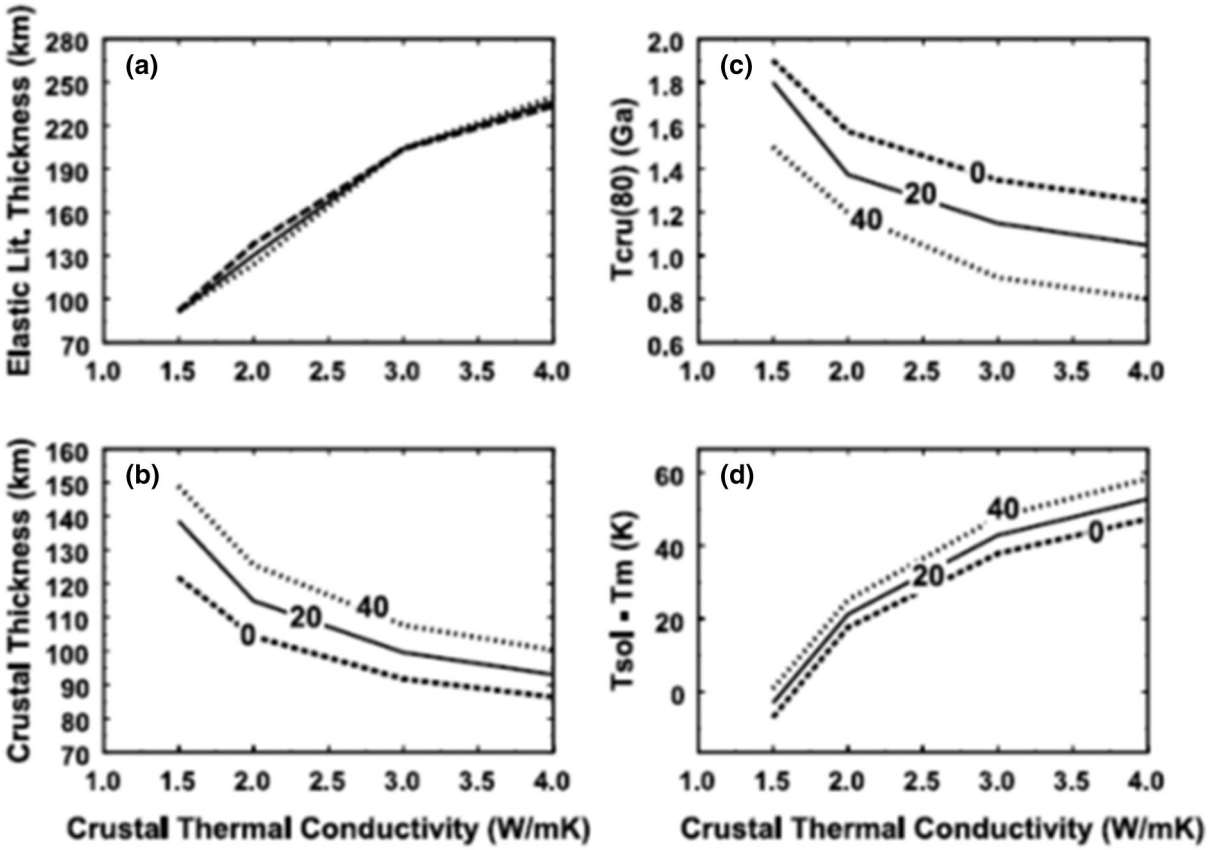

Fig. 4. Outputs for models from the work of Schumacher and Breuer (2006) for a range of crustal thermal conductivity inputs. The outputs are (a) present-day elastic lithosphere thickness (depth to 1050 K isotherm), (b) present-day crustal thickness, (c) time at which 80% of the crust has been formed, and (d) the present-day temperature difference between the solidus and the mantle. Primordial crustal thickness is adopted as 0, 20, and 40 km.

CONCLUSIONS

These new data are an improvement on the pre-existing data. While the measurements do not cover such low temperatures as previous work, they are direct measurements of thermal conductivity, with a larger number of data points, and are consistent with both theory and with extrapolations of well-established high-temperature curves. The data based on lunar samples are suspect, perhaps compromised by using powdered rock for the specific heat measurements, or by the presence of pores or microfractures, which would lead to lower figure for thermal conductivity. Calculating for the effects of porosity brings the lunar data closer to the new data but does not close the gap completely.

There are applications for these data in terrestrial (polar) geology and industry (thermo-fracking and underground cryogenic storage). Basalt at low temperatures is also common on planetary and meteoritic bodies; for example, around 10–20% of Mars' crust, and more at the poles, is in the temperature range of these data. While planetary crusts are more complex than bulk basalt, being fractured and porous, with the gaps in the rock being a vacuum, or filled with substances such as water ice, CO_2 ice, or clathrates, accurate data on the thermal conductivity of the crust's basalt component are important to any calculation of the bulk crust thermal conductivity. For lunar and meteoritic research, the usefulness of these data is limited by the temperature range, and by the effects of porosity and fracture, which is likely to be the determining factor for any calculation of the thermal conductivity.

The importance of using accurate thermal conductivity values in planetary science is shown by research in which models of Mars' thermal history are run with different values of the input crustal thermal conductivity (Schumacher & Breuer, 2006), the outputs of which are reproduced in Fig. 4. This shows that for an input average crustal thermal conductivity value of 2.0 W m^{-1} K^{-1}, a room temperature value used by many researchers to model Mars, the model output for the present-day crust is around 10 km thicker than if an input value of 2.5 W m^{-1} K^{-1} (i.e., 125 km rather than 115 km), was used.

Other parameters, affected by thermal conductivity, are also changed for small changes in the average crustal thermal conductivity. The elastic thickness of the lithosphere, the time to accrue 80% of the crust, and the temperature difference between the solidus and mantle temperature are all amended by 5–20% for a difference of 0.5 W m^{-1} K^{-1}.

Acknowledgments—The Theo's Flow basalt sample was supplied by courtesy of the University of Aberdeen's Geological Collection.

Data Availability Statement—Data sharing not applicable - All new data contained within manuscript.

Editorial Handling—Dr. Kevin Righter

REFERENCES

Arndt, N. T., and Nesbitt, R. W. 1982. Geochemistry of Munro Township Basalt. In *Komatiites*, edited by N. T. Arndt, and E. G. Nisbet, 309–29. London: George Allen & Unwin.

Beardsmore, G. R. and Cull, J. P. 2001. *Crustal Heat Flow: A Guide to Measurement and Modelling*. Cambridge, UK: Cambridge University Press.

Beck, A. E., and Beck, J. M. 1958. On the Measurement of the Thermal Conductivities of Rocks by Observations on a Divided Bar Apparatus. *Transactions of the American Geophysical Union* 39: 1111–23.

Çengel, Y. 2009. *Introduction to Thermodynamics and Heat Transfer*, vol. 2. New York: McGraw-Hill.

Churchill, S. W., and Chu, H. S. 1975. Correlating Equations for Laminar and Turbulent Free Convection from a Vertical Plate. *International Journal of Heat Mass Transfer* 18: 1323–9.

Clauser, C., and Huenges, E. 1995. Thermal Conductivity of Rocks and Minerals. In *Rock Physics & Phase Relations: A Handbook of Physical Constants*, edited by T. J. Ahrens, 105–26. Washington, D.C.: American Geophysical Union.

Clifford, S. M., Lasue, J., Heggy, E., Boisson, J., McGovern, P., and Max, M. D. 2010. Depth of the Martian Cryosphere: Revised Estimates and Implications for the Existence and Detection of Subpermafrost Groundwater. *Journal of Geophysical Research* 115: E07001.

Frolec, J., Králík, T., Musilová, V., Hanzelka, P., Srnka, A., and Jelínek, J. 2019. A Database of Metallic Materials Emissivities and Absorptivities for Cryogenics. *Cryogenics* 97: 85–99.

Fujii, N., and Osako, M. 1973. Thermal Diffusivity of Lunar Rocks Under Atmospheric and Vacuum Conditions. *Earth and Planetary Science Letters* 18: 65–71.

Gubareff, G. G., Janssen, J. E., and Torborg, R. H. 1960. *Thermal Radiation Properties Survey: A Review of the Literature*. Minneapolis: Honeywell Research Center.

Haenel, R., and Zoth, G. 1973. Heat Flow Measurements in Austria and Heat Flow Maps of Central Europe. *Zeitschrift für Geophysik* 39: 425–39.

Hobbs, P. V. 1974. *Ice Physics*. Oxford: Clarendon.

Horai, K., Simmons, G., Kanamori, H., and Wones, D. 1970. Thermal Diffusivity and Conductivity of Lunar Material. *Science* 167: 730–1.

Horai, K. 1971. Thermal Conductivity of Rock-Forming Minerals. *Journal of Geophysical Research* 76: 1278–308.

Horai, K., and Fujii, N. 1972. Thermophysical Properties of Lunar Material Returned by Apollo Missions. *The Moon* 4: 447–75.

Kadoya, K., Matsunaga, N., and Nagashima, A. 1985. Viscosity and Thermal Conductivity of Dry Air in the Gaseous Phase. *Journal of Physical and Chemical Reference Data* 14: 947.

Kanamori, H., Nur, A., Chung, D., Wones, D., and Simmons, G. 1970. Elastic Wave Velocities of Lunar Samples at High Pressures and Their Geophysical Implications. *Science* 167: 726–8.

Kravchenko, Y., and Krupskii, I. 1986. Thermal Conductivity of Solid N_2O and CO_2. *Soviet Journal of Low Temperature Physics* 12: 46–8.

Lentz, R. C. F., McCoy, T. J., Collins, L. E., Corrigan, C. M., Benedix, G. K., Taylor, G. J., and Harvey, R. P. 2011. Theo's Flow, Ontario, Canada: A Terrestrial Analog for the Martian Nakhlite Meteorites. In *Analogs for Planetary Exploration*, edited by W. B. Garry, and J. E. Bleacher. Boulder, Colorado: Geological Society of America.

LSPET (Lunar Sample Preliminary Examination Team). 1969. Preliminary Examination of Lunar Samples from Apollo 11. *Science* 165: 1211–27.

Macke, R. J., Britt, D. T., Consolmagno, G. J., and Hutson, M. L. 2010. Enstatite Chondrite Density, Magnetic Susceptibility and Porosity. *Meteoritics & Planetary Science* 45: 1513–26.

Marovelli, R. L., and Veith, K. F. 1965. Thermal Conductivity of Rock: Measurement by the Transient Line Source Method. Bureau of Mines Report of Investigations 6604, U.S. Department of the Interior.

McSween, H. Y. 2015. Petrology on Mars. *American Mineralogist* 100: 2380–95.

Nagao, T., and Kaminuma, K. 1986. Long-Term Underground Temperature Measurements at Syowa Station, East Antarctica. *Journal of Geodynamics* 6: 297–308.

Opeil, C. P., Consolmagno, G. J., Safarik, D. J., and Britt, D. T. 2012. Stony Meteorite Thermal Properties and Their Relationship with Meteorite Chemical and Physical States. *Meteoritics & Planetary Science* 47: 319–29.

Robie, R. A., Hemingway, B. S., and Wilson, W. H. 1970. Specific Heats of Lunar Surface Materials from 90 to 350 Degrees Kelvin. *Science* 167: 749–50.

Robie, R. A., and Hemingway, B. S. 1971. Specific Heats of the Lunar Breccia (10021) and Olivine Dolerite (12018) Between 90 and 350 Kelvin. Proceedings, 2nd Lunar Science Conference. pp. 2361–5.

Sass, J. H., Lachenbruch, A. H., Moses, T. H., and Morgan, P. 1992. Heat Flow from a Scientific Research Well at Cajon Pass, California. *Journal of Geophysical Research* 97: 5017–30.

Schumacher, S., and Breuer, D. 2006. Influence of a Variable Thermal Conductivity on the Thermochemical Evolution of Mars. *Journal of Geophysical Research* 111: E02006.

Seipold, U. 1998. Temperature Dependence of Thermal Transport Properties of Crystalline Rocks—A General Law. *Tectonophysics* 291: 161–71.

Sloan, E. D. 1997. *Clathrate Hydrates of Natural Gases*, 2nd ed. New York: Marcel Dekkar Inc.

Touloukian, Y. S., Powell, R. W., Ho, C. Y., and Nicolaou, M. C. 1970. *Thermophysical Properties of Matter, Thermal Conductivity: Nonmetallic Solids*, vol. 2. New York, NY: Plenum. Table 31R.

Tritt, T., ed. 2012. *Thermal Conductivity: Theory, Properties, and Applications*. Dordrecht: Kluwer.

Zoth, G., and Haenel, R. 1988. Appendix. *Handbook of Terrestrial Heat-Flow Density Determination. Solid Earth Sciences Library*, vol. 4, edited by L. Rybach, and L. Stegena. Dordrecht: Kluwer.